Inclusive pion scattering in the Δ(1232) region

S. M. Levenson,* D. F. Geesaman, E. P. Colton, R. J. Holt, H. E. Jackson, J. P. Schiffer, J. R. Specht, K. E. Stephenson,† and B. Zeidman
Argonne National Laboratory, Argonne, Illinois 60439

R. E. Segel
Northwestern University, Evanston, Illinois 63301

P. A. M. Gram
Los Alamos National Laboratory, Los Alamos, New Mexico 87545

C. A. Goulding‡
Florida A & M University, Tallahassee, Florida 32306

(Received 7 January 1983)

A systematic study of inclusive pion scattering from targets of ^{4}He, ^{12}C, ^{58}Ni, and ^{208}Pb has been performed at incident π^+ kinetic energies of $T_{\pi^+}=100$, 160, 220, and 300 MeV. Particular attention was paid to the kinematic region where energy losses were greater than typical single-particle binding energies. The spectra of scattered pions were integrated to yield angular distributions and total inelastic-scattering cross sections. The spectra for all targets are similar, showing a peak near that expected for a single-step quasifree scattering process.

[NUCLEAR REACTIONS ^{4}He, ^{12}C, ^{58}Ni, ^{208}Pb, $(\pi^+,\pi^{+\prime})$, $T_{\pi^+}=100$, 160, 220, 300 MeV; measured $d^2\sigma/d\Omega_{\pi^{+\prime}}dE_{\pi^{+\prime}}$.]

I. INTRODUCTION

The present experiment studied the systematic properties of inclusive pion scattering spectra using incident pions in the Δ(1232) energy region from a variety of nuclear targets. The kinematic region of pion energy losses greater than typical single-particle binding energies occupies a substantial fraction of the reaction cross section; therefore, measurements of the basic properties of this region are essential to a more complete understanding of how pions propagate in nuclei. Previous studies of inelastic scattering tended to be either exclusive experiments dealing with final states making up a small fraction of the inelastic yield,[1,2] or were taken using one or two targets, sometimes over a rather limited kinematic regime,[3–5] or were low-resolution cloud chamber and emulsion experiments.[6–8] The present study covers a wide range of targets, incident energies, and scattering angles with moderate resolution to provide a basis for determining the important reaction mechanisms. An earlier paper on this experiment presents some preliminary results, with emphasis on comparisons between ^{4}He and other nu-

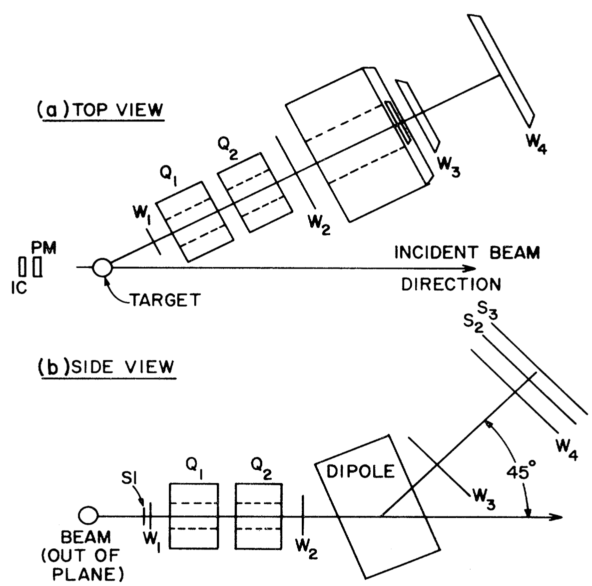

FIG. 1. The QQD spectrometric used in the present measurements is shown in top (a) and sited (b) view 5. The mean flight path through the spectrometer, from $S1$ to $S3$ was 5.3 m. The scintillators have been omitted from the top view for clarity.

TABLE I. Spectrometer characteristics.

Typical resolutions (FWHM at 300 MeV/c)	
Momentum	1%
Scattering angle	5 mr
Position on target	<1 cm
Momentum bite	25%
Angular bite	
vertical	90 mr
horizontal	280 mr

clei.[9] The purpose of the present paper is to make available more complete data, consisting of spectra, angular distributions, and total inelastic cross sections.

II. EXPERIMENTAL APPARATUS

The P^3 channel at the Los Alamos Meson Physics Facility (LAMPF) provided an incident pion beam of 10^6–10^7 pions/sec in the kinetic energy region from $T_{\pi^+} = 100$–300 MeV.[10] The beam spot on target was typically 2 cm (FWHM) in diameter, the beam momentum spread was $\pm 1.5\%$ (FWHM). An argon ion chamber upstream from the target continuously monitored the beam flux during the experiment.

To carry out the present measurements in a reasonable amount of beam time, it was necessary to construct a new, moderate resolution, large-acceptance QQD magnetic spectrometer, described in detail elsewhere.[11] The design and important characteristics of the spectrometer are shown in Fig. 1 and Table I, respectively. The mean flight path was 5.3 m, corresponding to a pion survival fraction of 40% at 100 MeV/c, the lowest momentum measured here. A helium bag enclosing the pion flight path reduced somewhat the degradation of the resolution due to multiple scattering. Four x-y sensing wire chambers measured the trajectory of the pion, with three planes of scintillators providing timing information for particle identification and triggering.

The solid targets (384 mg/cm^2 ^{12}C, 574 mg/cm^2 ^{58}Ni, and 594 mg/cm^2 ^{208}Pb) were in the form of 6.4×10.2 cm slabs. The cryostatic ^{4}He target volume was a 30.5 cm long by 7.6 cm diam cylinder described in Ref. 12. Software cuts on the position on target of the scattered pion along with the relatively small beam spot eliminated background scattering from target support structures.

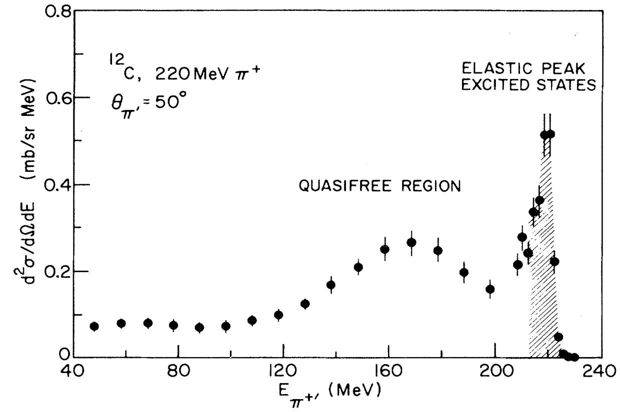

FIG. 2. A typical inelastic spectra from a ^{12}C target is shown. The shaded area was eliminated from the energy integration to approximately obtain the inelastic cross section $d\sigma/d\Omega$.

III. DATA ANALYSIS

For each event, the position on target, the scattering angles (θ and ϕ), and the momentum, were derived from the wire chamber coordinates using a least-squares fitting procedure, described in Ref. 11. A cut on the trajectory consistency value from this

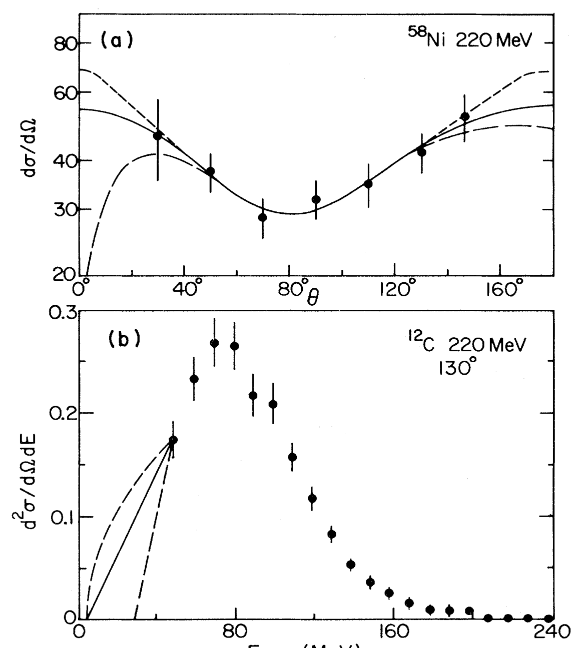

FIG. 3. The extrapolation used in estimating the integrated cross sections are shown. In (a) the area under the four term Legendre polynomial fit to the data represented by the solid line was taken as $\sigma_{\rm inel}$. In (b) the area under the data points and the solid line was taken as $d\sigma/d\Omega$. The dashed lines are reasonable estimates of possible errors.

TABLE II. Data. (All data taken using π^+'s.)

Target	Energies (in MeV)	Angles (in degrees lab)
^{12}C	100, 160, 220	30°–146° in 20° increments
	300	30°–120° in 30° increments
^{58}Ni, ^{208}Pb	100, 160, 220	30°–146° in 20° increments
^{16}O	100	30°–146° in 20° increments
^{4}He	100, 160, 220	30°–146° in 30° increments

procedure reduced the muon contamination in $d\sigma/d\Omega$ to less than 4%. Protons were easily differentiated from pions on the basis of time-of-flight measurements. Positrons, primarily from pair production following (π^+,π^0) reactions, were estimated to contribute less than 1% to the final spectra. A typical spectrum, as shown in Fig. 2, consists of four-momentum bites of 20% each, averaged over a $\pm 4°$ scattering-angle bite and overlapped by 5% in momentum as a consistency check. Corrections were made for the dead time, the pion-survival fraction, the momentum-dependent acceptance of the spectrometer, and energy loss in the target. Backgrounds measured using the empty cryostat were subtracted from the ^{4}He data. The absolute normalization of the incident pion flux was obtained by measuring π^+-p scattering and comparing to known values.[13,14] A polyethylene target was used in measuring this normalization for the solid targets, and a Styrofoam cylinder of the same dimensions as the cryostat target volume was used for normalizing the ^{4}He data. The overall normalization error is approximately 15%, point-to-point errors in the spectra are about 10%. To obtain inelastic angular distributions it was necessary to extrapolate the spectra to zero cross section at the Coulomb barrier. Additional extrapolations were made in integrating the angular distributions to obtain total inelastic cross sections. Examples of these extrapolations with estimates of errors are shown in Fig. 3. The integration of the spectra was carried out over the region of energy losses greater than 5 MeV to approximately exclude the elastic peak, as indicated in Fig. 2.

Table II contains a listing of targets, angles, and incident pion energies for which data were obtained. Spectra for all targets at $T_{\pi^+}=160$ and 220 MeV are shown in Figs. 4 and 5. Inclusive inelastic angular distributions for $T_{\pi^+}=160$ and 220 MeV are displayed in Fig. 6. The total integrated cross sections for inelastic scattering are shown in Table III and Fig. 7. Numerical tabulations of differential cross sections for all energies and targets are available on microfilm.[15]

IV. DISCUSSION OF DATA

A striking feature of the inelastic spectra is the presence of a broad peak which moves to lower energy at larger angles. This peak follows the trend of the free π-N elastic peak; the free π-N energy is indicated by arrows on the spectra shown in Fig. 4. This feature dominates the scattered pion inelastic spectra at $T_{\pi^+}=160$, 220, and 300 MeV. It is suggestive of a single-step π-N scattering process, where the width of the peak could be attributed to the Fermi motion of the nucleons. Previous measurements have shown similar quasifree behavior for ^{4}He at $T_{\pi^+}=90$–320 MeV and $\theta_{\pi^\pm}=30°$–135° (Ref. 3), ^{16}O at $T_{\pi^+}=115$, 165, and 240 MeV, $\theta_{\pi^{+\prime}}=30°$–134° (Ref. 4), and ^{12}C, ^{40,44,48}Ca at $T_{\pi^+}=180$ and 290 MeV, $\theta_{\pi^{+\prime}}=60°$ and 120° (Ref. 5). Our measurements show that this behavior is common to a wide variety of nuclei, from ^{4}He to ^{208}Pb, over a scattering angle range of $\theta_{\pi^{+\prime}}=30°$–146°.

The reaction mechanism seems to be rather insensitive to the details of nuclear structure. The spectra shown in Figs. 4 and 5 are similar in shape from ^{12}C to ^{208}Pb. A significant difference in the spectral shapes occurs at 50°, where the ^{12}C data seems more forward peaked and to have a proportionally smaller low-energy tail. The ^{4}He spectra also show a characteristic quasifree peak. This peak is somewhat narrower than that found for the heavier nuclei. Kinematic and nuclear structure considerations may be responsible for this difference.

Figure 8 shows a simple plane-wave impulse approximation calculation normalized to the ^{12}C data at $T_{\pi^+}=160$ MeV. This normalization is angle dependent, the calculation does not reproduce the magnitude or shape of the angular distributions. Here, the nucleus is assumed to be a degenerate Fermi gas, with a 221-MeV/c Fermi level, a value used in fitting 500 MeV/c inclusive electron scattering measurements.[16] The free π-nucleon T matrix as

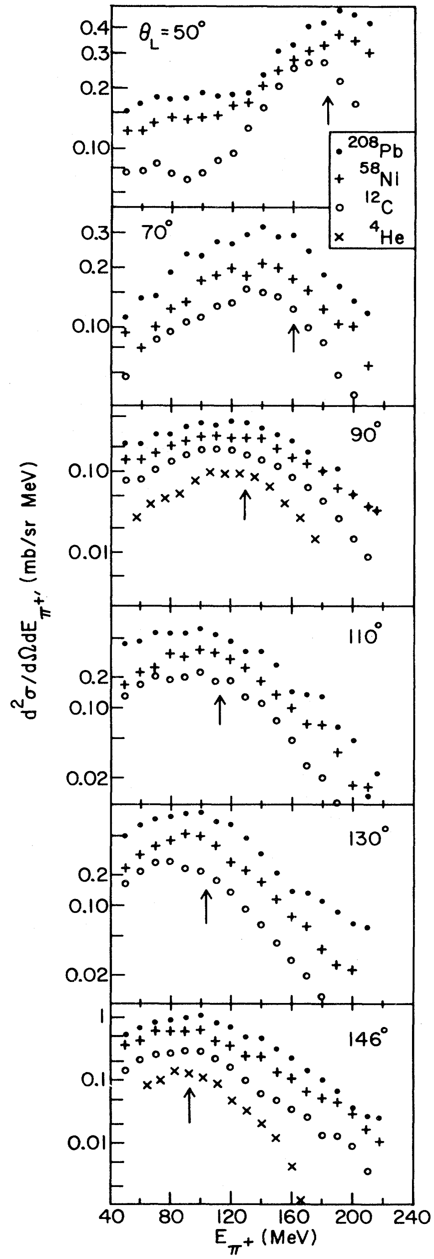

FIG. 4. The inelastic spectra at $T_{\pi^+} = 220$ MeV are shown. The elastic peak and low-lying excited states have been suppressed in this figure. (Energy losses <5 MeV are excluded.)

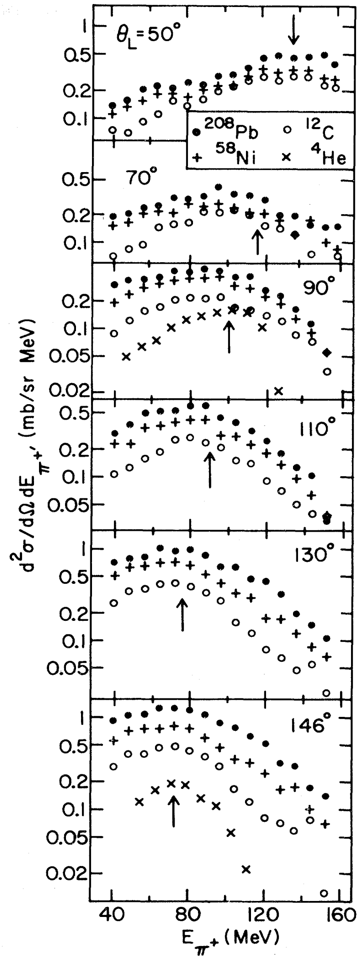

FIG. 5. The inelastic spectra at $T_{\pi^+} = 160$ MeV are shown with the elastic peak suppressed as in the preceding picture.

parametrized by Landau and Salomon[17] is employed. This calculation reproduces the width of the spectra rather well, and considering that it ignores all binding energy effects, it gives a reasonable value for the peak position. The effects of elastic scattering and absorption are ignored so that it is not surprising that the angular distribution is not reproduced in this calculation. Recently, more sophisticated calculations, using the isobar hole model and including medium corrections to the π-N t matrix, have been carried out for ^{4}He (Ref. 3) and ^{16}O (Ref. 18). Good agreement with the shape and magnitude of the quasifree region was obtained for incident energies of 163 MeV and greater. The interaction of the Δ with the rest of the nucleus is claimed to be an important factor in these calculations. To date, these calculations have only been applied to light nuclei. The similarity of the spectra for all nuclei observed in the present data suggests that such models may also be applicable to heavier nuclei.

Previously, it was noted that the π-nuclear angular distributions at back angles are rather similar from target to target and bear a strong resemblance to the free π^+-p angular distribution.[19–21] As shown in Fig. 6, the present π-nuclear angular distributions are roughly consistent with the shape of the free π^+-p distributions. However, there seems to

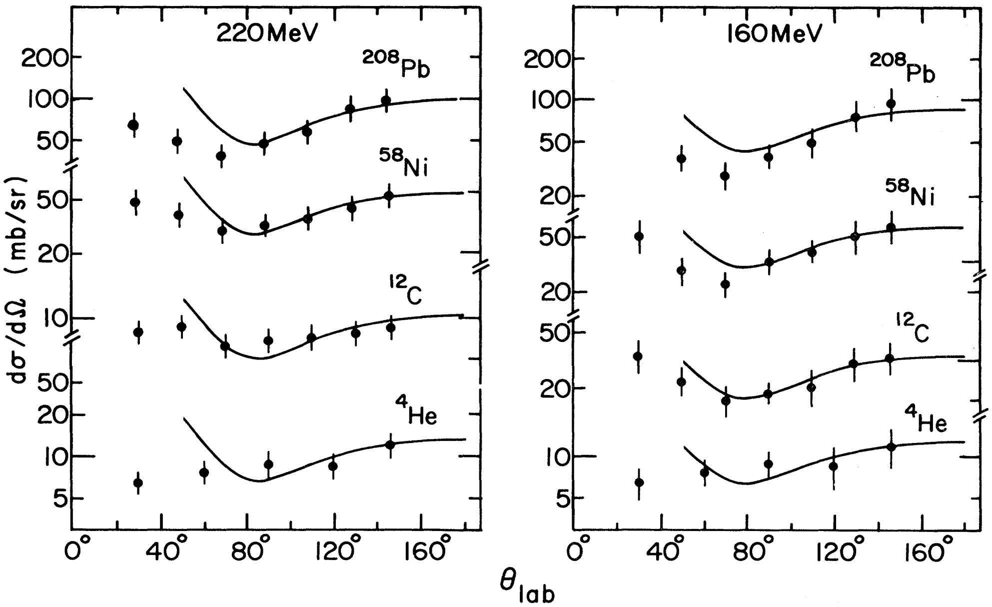

FIG. 6. Inelastic angular distribution at $T_{\pi^+}=160$ and 220 MeV are shown. The solid lines are the free π^+p cross sections normalized to the data.

be a trend towards a steeper backward angular distribution on heavier nuclei. At forward angles, the π-nucleus distributions rise slower than those for π-N scattering. This may in part be due to the Pauli blocking of low-momentum transfer events; the momentum transfer to the struck nucleon must be great enough to excite it to an unoccupied state. The tight binding and lack of excited states in ^{4}He seem to enhance this effect. Geometric shadowing effects would also tend to suppress forward quasifree scattering.

It has proven useful to express the various components of the reaction cross section as power laws in A to make clear the gross behavior of these channels. As shown in Fig. 7, the inelastic cross sections measured in the present experiment rise as A^N, where $N=0.40\pm0.09$ averaged over all energies and excluding ^{4}He. Previous values obtained for this exponent using positive pions in the resonance region are $N=0.45\pm0.03$ by McKeown *et al.*[21] (here only the integrated yield over the backward hemisphere was considered), and $N=0.44\pm0.05$ by Ashery

TABLE III. Total inelastic cross sections. (Absolute errors are 30% at 100 and 300 MeV and 20% elsewhere.)

A	100 MeV	160 MeV	220 MeV	300 MeV
^{4}He	30	130	100	
^{12}C	150	280	240	169
^{58}Ni	310	470	500	

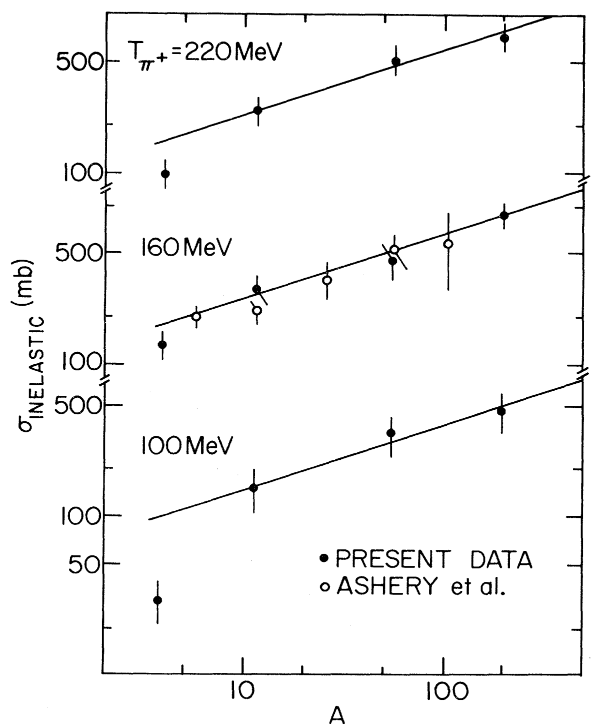

FIG. 7. The total inelastic cross sections are shown as a function of A. The solid lines are proportional to $A^{0.4}$.

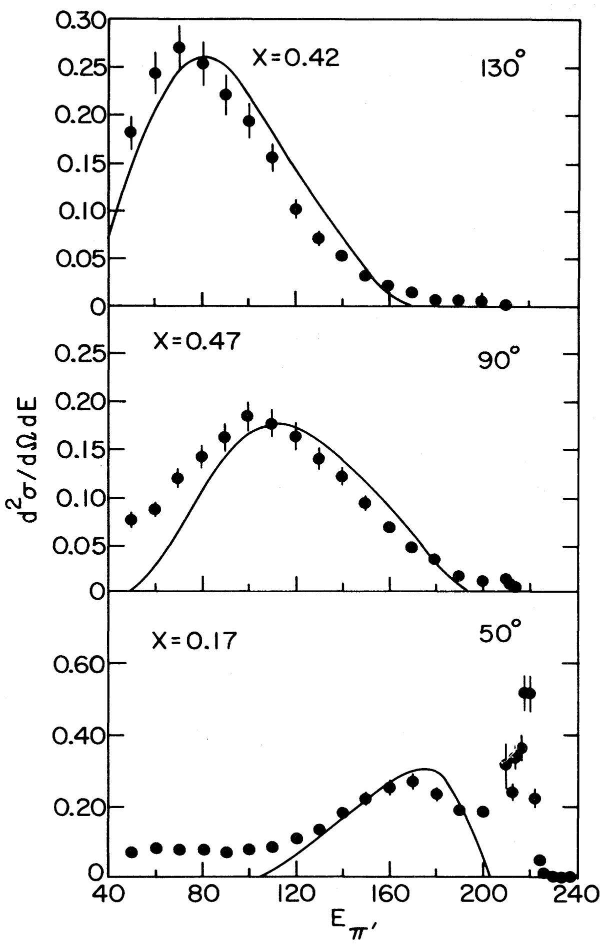

FIG. 8. The plane wave impulse approximation calculation, described in the text, is shown normalized to the ^{12}C data by the factor x.

et al.[20] As we also show in Fig. 7, the measurements of Ashery *et al.* at 165 MeV are consistent with the present values. An advantage of the present experiment is that the inelastic and elastic components of the spectra could be directly separated. All of these measurements are consistent with inelastic scattering increasing slower than the geometrically varying total reaction cross section with respect to A.

V. CONCLUSION

The inelastic spectra from the wide variety of targets studied here seem to be dominated by a single-step scattering mechanism. The specific details of the target nucleus have little effect on the gross features of the spectra. It has been suggested that absorption is responsible for suppressing multiple scattering, and thus enhancing the single-step fraction of the inelastic spectra. Measurements of exclusive processes, such as $A(\pi,\pi'N)$, may help lead to a more clear understanding of the various reaction mechanisms. Such experiments on ^{4}He are particularly important as the final-state interaction of the nucleon is minimized, thus simplifying the interpretation of the results.

This work was supported under the auspices of the Argonne National Laboratory (Laboratory-Graduate Fellowship), and sponsored by the Division of Educational Programs supported by the Department of Energy (DOE) under Contract W-31-109-Eng-38.

---

*Present address: Northwestern University, Evanston, IL 60204.
†Present address: EMR-Photoelectric, Princeton, NJ 08540.
‡Present address: EG & G Ortec, Los Alamos, NM 87544.

[1]B. J. Dropesky, G. W. Butler, C. J. Orth, R. A. Williams, G. Friedlander, M. A. Yates, and S. B. Kaufman, Phys. Rev. Lett. 34, 821 (1975).

[2]L. W. Swenson, T. Sharma, K. Krane, P. Varghese, D. K. McDaniels, H. A. Theissen, Noby Tanaka, M. Greenfield, and C. F. Moore, Phys. Rev. Lett. 40, 10 (1978).

[3]M. Baumgartner, H. P. Gubler, G. R. Plattner, W. D. Ramsay, H. W. Roser, I. Sick, P. Zupranski, J. P. Egger, and M. Thies, Phys. Lett. 112B, 35 (1982).

[4]C. H. Q. Ingram, *Meson-Nuclear Physics—1979 (Houston),* Proceedings of the 2nd International Topical Conference on Meson-Nuclear Physics, AIP Conf. Proc. No. 54, edited by E. V. Hungerford III (AIP, New York, 1979), p. 455.

[5]G. R. Burleson, G. S. Blanpied, J. Davis, J. S. McCarthy, R. C. Minehart, C. A. Goulding, C. L. Morris, H. A. Theissen, W. B. Cottingame, S. Greene, and C. F. Moore, Phys. Rev. C 21, 1457 (1980).

[6]Yu. R. Gismatullin, I. A. Lantsev, V. I. Ostrumov, and A. Ya. Smelynaskii, Yad. Fiz. 19, 45 (1974) [Sov. J. Nucl. Phys. 19, 22 (1974)].

[7]Ya. A. Berdnikov, Yu. R. Gismatullin, I. A. Lantsev, and V. I. Ostrumov, Yad. Fiz. 25, 490 (1977) [Sov. J. Nucl. Phys. 25, 265 (1977)].

[8]F. Balestera, M. P. Bussa, L. Busso, R. Garfagnini, G. Piragino, C. Guaraldo, A. Maggiora, R. Scrimaglio, I. V. Folomkin, G. B. Pontecorvo, and Yu. Scherbakov, Nucl. Phys. A340, 372 (1980).

[9]S. M. Levenson, D. F. Geesaman, E. P. Colton, R. J.

Holt, H. E. Jackson, J. P. Schiffer, J. R. Specht, K. E. Stephenson, B. Zeidman, R. E. Segel, P. A. M. Gram, and C. A. Goulding, Phys. Rev. Lett. 47, 479 (1981).

[10]R. D. Werbeck and R. J. Macek, IEEE Trans. Nucl. Sci. NS-22, 1598 (1975).

[11]E. Colton, Nucl. Instrum. Methods 178, 95 (1980).

[12]H. E. Jackson, S. L. Tabor, K. E. Rehm, J. P. Schiffer, R. E. Segel, L. L. Rutledge, and M. A. Yates, Phys. Rev. Lett. 39, 1601 (1977).

[13]P. J. Bussey, J. R. Carter, A. A. Carter, and A. M. Smith, Nucl. Phys. B58, 363 (1973).

[14]J. R. Carter, D. V. Bugg, and A. A. Carter, Nucl. Phys. B58, 378 (1973).

[15]See AIP document No. PAPS PRVCA-28-326-19 for 19 pages of tabulations of $d^2\sigma/d\Omega\, dE$, $d\sigma_{\rm inel}/d\Omega$, and $\sigma_{\rm inel}$. Order by PAPS number and journal reference from American Institute of Physics Auxiliary Publication Service, 335 E. 45 St., New York, N.Y. 10017. The price is $1.50 for microfiche, or $5 for photocopies. Airmail additional. Make check payable to American Institute of Physics.

[16]E. J. Moniz, I. Sick, R. R. Whitney, J. R. Ficenec, R. D. Kephart, and W. P. Towner, Phys. Rev. Lett. 26, 445 (1971).

[17]R. Landau and M. Salomon, TRIUMF report (unpublished).

[18]Michael Thies, Nucl. Phys. A382, 434 (1982).

[19]I. Navon, D. Ashery, G. Azuelas, H. K. Walter, and F.W. Schleputz, Phys. Rev. C 22, 717 (1980).

[20]D. Ashery, I. Navon, G. Azuelas, H. K. Walter, and F. Schleputz, Phys. Rev. C 23, 2173 (1981).

[21]R. D. McKeown, S. J. Sanders, J. P. Schiffer, H. E. Jackson, M. Paul, R. Specht, E. J. Stephenson, R. P. Redwine, and R. E. Segel, Phys. Rev. C 24, 254 (1981).